Absorption Spectra and Linear Dichroism of Some Amphibian Photoreceptors

FERENC I. HÁROSI

From the Laboratory of Neurophysiology, National Institute of Neurological Diseases and Stroke, National Institutes of Health, Bethesda, Maryland 20014

ABSTRACT Absorption spectra and linear dichroism of dark-adapted, isolated photoreceptors of mudpuppies, larval and adult tiger salamanders, and tropical toads were measured microspectrophotometrically. Spectral half-band width, dichroic ratio, and transverse specific density were determined using averaged polarized absorptance spectra and photomicrographs of seven types of rod outer segments. Two classes of cells were found, one with higher specific density and dichroic ratio, associable with the presence of rhodopsins, the other, lower in both quantities, associable with porphyropsins. Relationships were derived to calculate the product of molar concentration and extinction coefficient ($c\epsilon_{max}$) from specific density and dichroic ratio. By utilizing the hypothesis of invariance of oscillator strengths and measured half-band widths, ϵ_{max} values were independently determined, permitting the calculation of c. The pigment concentration for all cells tested was about 3.5 mM. The broadness of green rod pigment spectra is correlated with reduced molar absorptivity and reduced cellular specific density. Estimation of physiological spectral sensitivities is discussed. Based on dichroic ratio considerations, a model is proposed for the orientation of retinals *in situ* which could account for the apparent degree of alignment of transition moments. In the chosen orientation, the ring portion of conjugation becomes primarily responsible for axial extinction. Reduced dichroism of dehydroretinal-bearing cells can thus result from the extended ring conjugation of chromophores. Some inferences derivable from the model are discussed.

INTRODUCTION

Although vertebrate photoreceptors possess remarkable functional and structural similarities among the many thousands of species, they also exhibit diversification in that any one of a number of visual pigments may be packed into the specialized "outer segment" region of a particular type of rod or cone cell. Consequently, it should come as no surprise that several differences in optical and spectroscopic properties have been observed between dark-adapted goldfish cones and frog rods (Hárosi and MacNichol, 1974 *a*, *b*). For one, the outer segments of goldfish cones yield lower values of transverse specific density (the optical density for transversely polarized light per micrometer thickness) than the corresponding parts of frog rods. Also, the outer

segments of goldfish cones yield lower dichroic ratios (the optical density of the cell at transverse polarization of light divided by the optical density at axial polarization) as compared with frog rods when both are determined at λ_{max} (the wavelength of peak absorption of visible light). Furthermore, the spectrum of the red-absorbing goldfish cone pigment is substantially narrower than that of the other goldfish cone pigments having λ_{max} at shorter wavelengths.

Hárosi and MacNichol (1974 *a*) noted that the observed lower specific density of goldfish cones was consistent with a lower molar extinction of visual pigments using the dehydroretinal chromophore (porphyropsins) than those utilizing retinal as chromophore (rhodopsins). At the same time, however, they were unable to explain the smaller linear dichroism in goldfish cones as compared with that in frog rods; nor could they exclude the possibility that geometrical factors, such as the smaller size and conical shape of goldfish cones, contributed to the cellular optical density measurements. It also remained questionable whether or not subtle differences in the submicroscopic architecture of rod and cone outer segments invalidated the direct comparison of their dichroism.

Hárosi and MacNichol (1974*a*) interpreted the narrowness of the red-absorbing cone pigment spectrum in terms of two basic assumptions: first, that the *in situ* visual pigment concentration is about the same in vertebrate photoreceptors, regardless of type, and second, that the oscillator strength associated with the main absorption band is approximately invariant within the same family of visual pigments. Thus, they linked the narrowing of the red-absorbing pigment spectrum to a corresponding increase in molar absorptivity. Although the calculated gain of about 30% in molar extinction for the red-absorbing goldfish cone pigment was consistent with other observations, they failed to corroborate this result with measurements. For example, it was not demonstrated (because of the technical difficulties involved) whether there is a corresponding increase in specific density of outer segments containing the pigment with the narrower spectrum as compared with the specific density of cones whose pigment spectra match the standard shape of porphyropsin.

The present study was undertaken to compare several rhodopsins and porphyropsins *in situ* under more favorable conditions than formerly achieved. Therefore, large rod outer segments of the larval and adult tiger salamanders, tropical toad, and mudpuppy were selected which not only permitted more accurate experimental data acquisition but also eliminated the effects due to geometrical factors and other possible differences between rods and cones.

METHODS

Experimental Material

The animals used in this study were purchased from a commercial supplier (The Mogul Corp., Oshkosh, Wis.). They consisted of adult (28–35 cm long) mudpuppies

(*Necturus maculosus*), larval (18–24 cm long) tiger salamanders (*Ambystoma tigrinum*), and medium-to-large-size tropical toads (*Bufo marinus*). Adult salamanders (land phase) were acquired from the purchased larvae (aquatic phase) by spontaneous metamorphosis, a process usually requiring a few weeks. The mudpuppies were kept in a refrigerated aquarium (4–5°C) in the dark, whereas the salamanders and toads were kept at room temperature (21–23°C) and at normal laboratory illumination. Before sacrificing the animals for experimental use, they were kept in complete darkness for a few hours.

Preparation

Except for minor variations, the same procedure was followed as previously described (Hárosi and MacNichol, 1974 *a*). The dark-adapted animals were decapitated under dim red light, while enucleation, dissection of the eyes, and the removal of the retinas were done mostly under infrared illumination using a low-power dissecting microscope equipped with an image converter. Small retinal fragments were teased apart on a coverglass at room temperature in the presence of a salt solution containing 110 mM NaCl, 2 mM KCl, 2 mM $CaCl_2$, and 10 mM HEPES (*N*-2-hydroxyethylpiperazine-*N'*-2-ethanesulfonic acid) buffer at pH 7.4 for all the experiments in this series. By placing a second (smaller size) coverglass on top of the first, blotting off the excess fluid, and sealing the edges against evaporation, a glass sandwich was produced that constituted the preparation. A layer of liquid 20–30 μm deep existed in its interior which normally contained hundreds of photoreceptor fragments lying on their side, some of which were then selected for measurement under microscopic examination.

Measuring Apparatus

The polarized light absorption of single cells were recorded with the dichroic microspectrophotometer (DMSP), described most recently by Hárosi and MacNichol (1974 *b*) and Hárosi (1975 *a*). In its essential features, the instrument is a rapid, wavelength-scanning and recording, single-beam microspectrophotometer, capable of resolving absorptance into two simultaneous and mutually orthogonal components (designated $A_\perp$ and $A_\parallel$). These components correspond to absorption of light polarized across and along the long dimension of the slit-shaped cross section of the beam, with polarization defined by the plane of vibration of the electric vector associated with the light wave.

The instrument is equipped with a small, on-line digital computer whose stored program controls its operation at all times. During its automatically repeating spectral scanning, the computer sums photocurrents of corresponding wavelength regions of all scans in 75 sampling bins. The sums thus obtained, proportional to the average values of polarized transmitted light fluxes along the spectrum, serve in the computation of the polarized components of absorptance as follows:

$$A_\perp(\lambda) = 1 - \Phi_\perp(\lambda)/\Phi'_\perp(\lambda),$$

and

$$A_\parallel(\lambda) = 1 - \Phi_\parallel(\lambda)/\Phi'_\parallel(\lambda),$$

where $\Phi_{\perp}(\lambda)$ and $\Phi_{\parallel}(\lambda)$ are the transmitted polarized fluxes measured through a receptor and $\Phi'_{\perp}(\lambda)$ and $\Phi'_{\parallel}(\lambda)$ are the transmitted polarized fluxes measured through a clear region of the preparation. It is assumed in the above relationships that all light removed from the measuring beam by the receptor is due to the spectral absorption of its pigment and that a negligible amount of light is reflected, refracted, or scattered outside the beam. This appears to be justifiable in thin preparations and when a large numerical aperture objective is utilized to collect the light.

Procedure of Measurement

The experiments were carried out at room temperature (21–23°C) during the months of June and July, 1974. The illustrations were produced by averaging chosen spectra out of a total of 91 single-cell experiments, each consisting of 32 full scans of the spectrum (during which the wavelength of light was alternately varied from red to blue and from blue to red, between 322.5 and 697.5 nm, at a constant rate of 500 nm/s). The flux density of the measuring beam was previously determined (Hárosi and MacNichol, 1974 *b*) to be approximately 2×10^{13}–7×10^{13} quanta/cm^{2}s in the wavelength range of 400–700 nm. Such a flux of light under usual experimental conditions and during a 32-scan measurement was found to bleach 6–7% of a goldfish cone pigment and 9–10% of a frog rod pigment (Hárosi and MacNichol, 1974 *a*, *b*). Thus, in the estimation of initial pigment concentrations, the measured peak densities were corrected by increasing their values by 10% in the case of rhodopsin-bearing cells and by 7% in the case of porphyropsin-bearing cells. The geometrical extent of the beam in the plane of the specimen was about 3×20 μm, achieved by demagnifying the opening of an adjustable rectangular diaphragm by the condenser used (Carl Zeiss, Inc., Oberkochen, W. Germany, Ultrafluar, 32×, numerical aperture = 0.4). The objective of the DMSP was of the same series but had a larger numerical aperture (Ultrafluar, 100×, numerical aperture = 0.85). For the underlying reasons of these choices, see discussions by MacNichol et al. (1973) or by Hárosi (1975 *a*).

The measurements commenced as soon as the preparation was readied and usually continued for 2–3 h thereafter. The glass sandwich, affixed to the gliding stage of the microscope of the DMSP, was moved in search of photoreceptor outer segments at dim red illumination. When an appropriate cell was found, the axis of the outer segment was aligned with the long dimension of the slit (reference direction), after which an initial reference measurement was recorded through a clear area near the cell. The transmitted light through the cell was then recorded and both sets of data punched on paper tape for permanent records before proceeding to the next measurement. Off-line data analysis consisted of further averaging of the 32-scan spectra (Hárosi and MacNicholl, 1974 *b*). The mean results were finally displayed on an oscilloscope face as well as listed numerically point by point, the former being photographed for illustrations and the latter used in subsequent computations.

Standard Curves

Standard extinction (optical density) curves with which to compare the experimental spectra were derived from the rhodopsin data of Dartnall (1967 *a*) and the porphyropsin data of Bridges (1967). The use of these data as standards is based on the principle

(generalized from the empirical findings of Dartnall, 1953) that the shape of the curve relating relative extinction to wave number (the reciprocal of wavelength) is approximately invariant for visual pigments having the same chromophore, regardless of λ_{max}. Bridges (1965, 1967) demonstrated that this relationship holds true for porphyropsins as well (with λ_{max} ranging from 521 to 543 nm), although the curve is broader than that established to match many rhodopsins.

Dartnall's "new nomogram" was used to generate rhodopsin-type standard curves for λ_{max} = 500, 502, 504, 506, 431, 433, 435, and 437 nm as follows. (*a*) The wavelengths λ_x corresponding to the relative extinctions (absorption coefficients) and wave number steps k_x given in Table 7.9 (Dartnall, 1967 *a*) were calculated from the formula $k_x = (10^7/\lambda_x) - (10^7/\lambda_{max})$, where λ_{max} is the chosen peak wavelength in nanometers. (*b*) The wavelength vs. relative extinction pairs thus obtained were linearly interpolated for integer wavelengths at 10-nm intervals. (*c*) The resulting relative extinctions were scaled, rounded off to nearest integers, and made available in digital form (on paper tape) for eventual computer displaying. The porphyropsin template was prepared in a similar manner, based on the approximated absorption spectrum of a porphyropsin with λ_{max} = 523 nm as compiled by Bridges (1967, Table 5, Columns IV and V). The template for the red rod pigment spectrum of the larval salamander was constructed by trial-and-error computer simulation. By assuming the presence of a mixture of rhodopsin (λ_{max} = 502 nm) and porphyropsin (λ_{max} = 523 nm), the experimental spectrum was found to be best approximated by a normalized sum of extinctions in which the proportion is 6 to 1 in favor of porphyropsin.

The half-band width of a measured spectral component was determined as follows. (*a*) The absolute optical density of the maximum D_{max} was calculated from the peak absorptance value A_{max} by the relation $D_{max} = \log_{10} (1 - A_{max})^{-1}$. (*b*) The wavelengths (λ_1, λ_2) corresponding to the 50% density value on the slopes of the relative absorptance curve (determined from the expression $A_\nu = 1 - 10^{-0.5D_{max}}$) were identified on the photographically enlarged record. (*c*) The half-band width in reciprocal centimeters (cm^{-1}) was calculated from the formula $\Delta\nu = |(10^7/\lambda_1) - (10^7/\lambda_2)|$, where λ_1 and λ_2 were expressed in nanometers.

RESULTS

Necturus maculosus

Crescitelli (1958) succeeded in extracting a visual pigment from the retina of mudpuppy. The alkaline difference spectra to partial bleaches yielded maximum density losses at about 526 nm and increases in peak density at about 405 nm, irrespective of the color of the bleaching light. Because hydroxylamine difference spectra of its solutions yielded maximum density losses at 522 nm and peak density gains at 388 nm, the pigment was identified as a porphyropsin. Although Brown et al. (1963) designated the absorption maximum of porphyropsin in this retina to be 525 nm and Liebman (1972) placed the λ_{max} at 527 nm, the present study yields 523 ± 1 nm as the λ_{max} of the *Necturus* rod pigment, in close agreement with Crescitelli's result.

Average transverse absorption characteristics of isolated *Necturus* rods are shown in Fig. 1. From part *a*, the dichroic ratio was found to be 3.12 at λ_{max}. The actual value of λ_{max} was determined by visual comparison of the measured components with the porphyropsin template. In part *b*, a good fit appears between the λ_{max} = 523-nm standard and the transverse component. The slight broadening of $A_\perp$ below 500 nm is probably due to a transversely dichroic product of bleaching (presumably metaporphyropsin II with $\lambda_{max} \simeq 405$ nm). This explanation is supported by the fact that the axial component $A_\parallel$ depicted in part C does not show any broadening. The spectral half-band widths were

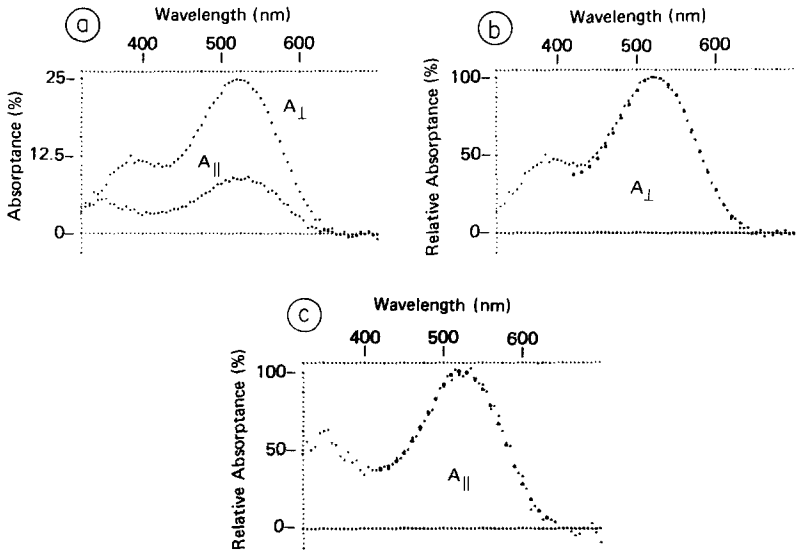

FIGURE 1. Polarized light absorption by transversely oriented dark-adapted rod outer segments of the mudpuppy (*N. maculosus*). (*a*) The average of 10 single-cell recordings, each consisting of 32 bidirectional spectral scans. (*b*) The normalized transverse component (small filled circles) and a standard curve of 523-nm peak (large filled circles) based on the data of Bridges (1967). (*c*) Same as *b*, except the axial component.

found to be near 4,800 cm^{-1} for both components. The transverse specific density of *Necturus* rods was determined to be 0.0128/μm (assuming that the average cell diameter is the proper path length through which the measuring light travels within the cells).

Ambystoma tigrinum (*Aquatic Phase*)

Although the tiger salamander might be expected to possess the same visual pigments as the frog (*Rana pipiens*) based on a brief statement by Liebman (1972), the situation turns out to be more complicated. Lasansky and Mar-

chiafava (1973, personal communication) noted, while recording the electrical responses elicited by light from larval tiger salamander photoreceptors, that the presumed rod responses peak at about 515 instead of the 502 nm which would be expected of cells using frog rhodopsin. The records shown in Fig. 2 confirm their observations in that peak absorption of the red rod outer segments takes place near 516 nm. It appears relevant to recall the discovery of Wald (1945) that the bullfrog tadpole yields visual pigment extracts with λ_{max} = 516 nm, which he interpreted to be due to the presence of "porphyropsin mixed with a little rhodopsin." Crescitelli (1958, 1972) not only confirmed Wald's value of λ_{max} but also established (by using the method of partial bleaching) the ratio of porphyropsin to rhodopsin to be 7.3 to 1 in the bullfrog tadpole retinal extracts. In view of these previous results, it was assumed, for the purpose of interpretation of λ_{max} and spectral shapes, that a similar

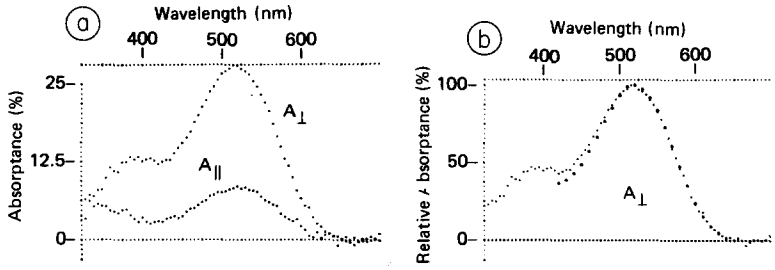

FIGURE 2. Polarized light absorption by transversely oriented dark-adapted red rod outer segments of the larval tiger salamander (*A. tigrinum*). (*a*) The average of 11 single-cell recordings, each consisting of 32 bidirectional spectral scans. (*b*) The normalized transverse component (small filled circles) and a standard curve of about 516-nm peak (large filled circles) constructed from porphyropsin (λ_{max} = 523 nm) and rhodopsin (λ_{max} = 502 nm) standard curves weighted in a ratio of 6 to 1 (see Methods).

visual process prevails in the larval stage of salamander as in the bullfrog larvae, and the standard curve was constructed accordingly (see Methods).

Fig. 2 *a* shows the average polarized absorption components of the larval salamander red rods, which strongly resemble those of the *Necturus* rods. The match between the transverse component and the template (with λ_{max} = 516 ± 2 nm) is illustrated in part *b*, showing good agreement between the two. The broadening of $A_\perp$ with respect to the standard below 500 nm is again ascribed to photoproduct absorption by the foregoing argument. The half-band widths of the two components were found to be about 4,900 cm^{-1}, the average dichroic ratio at 515–520 nm, 3.78, and the transverse specific density, 0.0120/μm.

The retina of the larval salamander is also populated, although sparsely, with thinner and somewhat shorter rods that can be identified as "green" on the basis of their blue-absorbing pigment content, as revealed by Fig. 3 *a*. The

normalized transverse component is compared to a rhodopsin template of λ_{max} = 433 nm in part *b*. The poor matching between the two traces is primarily due to the greater broadness of the measured spectrum, which may also be observed in the axial component (not illustrated). The half-band width of the green rod pigment spectrum of the larval salamander was estimated to be about 5,800 cm^{-1}, which is a value not only exceeding the breadth of a typical rhodopsin ($\Delta\nu \simeq 4{,}100$ cm^{-1}) or porphyropsin ($\Delta\nu \simeq 4{,}800$ cm^{-1}) but also becoming the broadest visual pigment spectrum ever so determined. Its extreme broadness hampers the effort of establishing its λ_{max}, for there are numerous ways of fitting the existing narrower templates to the broader curve. While the probable peak may be closer to 435 nm, it was designated to be 433 ± 4 nm, the larger tolerance implying the uncertainty of this method of

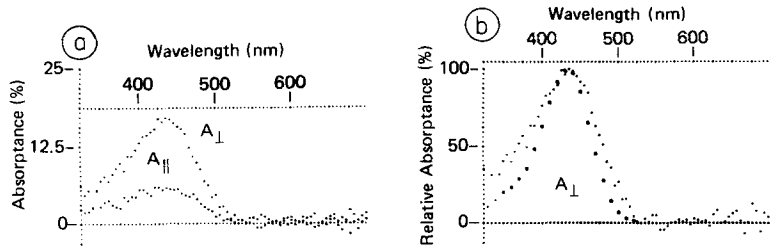

FIGURE 3. Polarized light absorption by transversely oriented dark-adapted green rod outer segments of the larval tiger salamander (*A. tigrinum*). (*a*) The average of two single-cell recordings, each consisting of 32 bidirectional spectral scans. (*b*) The normalized transverse component (small filled circles) and a rhodopsin standard curve of 433-nm peak (large filled circles).

identification. The average dichroic ratio at 435 nm was found to be 3.16 and the transverse specific density, 0.0115/μm.

Ambystoma tigrinum (*Land Phase*)

The adult tiger salamander appears to use visual pigments in its retinal rod cells that are spectroscopically indistinguishable from the rhodopsin-type rod pigments of most adult amphibia. The averaged components of red rod absorption spectra are shown in Fig. 4 *a*, with identifiable features of large transverse peak absorptance ($A_\perp$ = 0.329) and large peak dichroic ratio (R = 4.55). The match between the transverse component and the rhodopsin template (λ_{max} = 502 nm) is illustrated in part *b*. It is to be noted that the agreement between the two is deceptively good; if the experimental data were also represented by relative densities (extinctions) as are the standard data, then the measured spectrum would appear slightly narrower than the template. The half-band width determinations yielded nearly 4,000 cm^{-1} for the two experimental components and about 4,200 cm^{-1} for the standard curve. These figures com-

pare favorably with the 4,100-cm^{-1} width measured earlier in an extinction spectrum of cattle rhodopsin (cf. Table I, Hárosi and MacNichol, 1974 *a*). The average (uncorrected) transverse specific density of the adult salamander red rod outer segments was found to be 0.0177/μm.

The retina of the adult salamander, just as that of the larva, also has green rods. The average polarized absorption components are illustrated in Fig. 5 *a*. Although the normalized transverse component and the rhodopsin standard (λ_{max} = 433 nm), shown together in part *b*, are in closer agreement than the larval green rod spectrum and the same standard were, the match is still too loose to permit accurate λ_{max} determination. The half-band widths of the measured components were determined to be about 5,100 cm^{-1} and the dichroic ratio to be 3.49. The cellular specific optical density could not be established for lack of photographic information on cell dimensions.

Bufo marinus

Information concerning the visual cells and pigments of this tropical toad is scarce. While no anatomical description of its eye is readily available, its retina

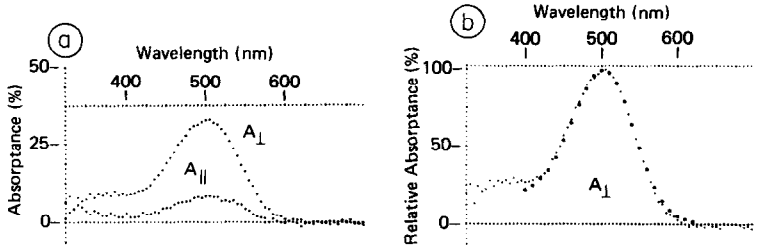

FIGURE 4. Polarized light absorption by transversely oriented dark-adapted red rod outer segments of the adult tiger salamander (*A. tigrinum*). (*a*) The average of six single-cell recordings, each consisting of 32 bidirectional spectral scans. (*b*) The normalized transverse component (small filled circles) and a standard curve of 502-nm peak (large filled circles) based on the data of Dartnall (1967 *a*).

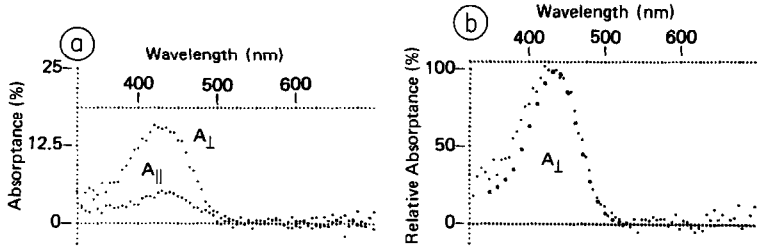

FIGURE 5. Polarized light absorption by transversely oriented dark-adapted green rod outer segments of the adult tiger salamander (*A. tigrinum*). (*a*) The average of two single-cell recordings, each consisting of 32 bidirectional spectral scans. (*b*) The normalized transverse component (small filled circles) and a rhodopsin standard curve of 433-nm peak (large filled circles).

has been extracted by Crescitelli (1958), who found the peaks of the alkaline difference spectrum at 502 and 375 nm and the peaks of the hydroxylamine difference spectrum at 503 and 368 nm. Because he obtained similar results with the retinal extracts of *R. pipiens* as well, the main visual pigments of *B. marinus* could be expected to be like those of *R. pipiens*.

The photomicrograph presented in Fig. 6 shows some of the photoreceptor cells of this toad as they appeared in the thin, teased retinal preparation of the DMSP. The rectangular images visible in the photograph were cylindrical rod outer segments. Their light-absorbing properties were found to be of two kinds, consistent with the presence of red and green rods in the amphibian retina. After the identification of their pigment content and the conspicuous correlation of shape and pigment type, the viewer should find no difficulty in accepting the opinion of Walls (1963) that the "green rod (of Schwalbe) is probably more cone-line than rod-like." In addition to their conical shape, the green rods of *Bufo* seem unique in their large diameter, exceeding those of the red rods by about 25%, which makes them desirable targets for single-cell work.

Polarized average absorption components of the red rod outer segments are shown in Fig. 7 *a*. As expected, they closely resemble the spectral components

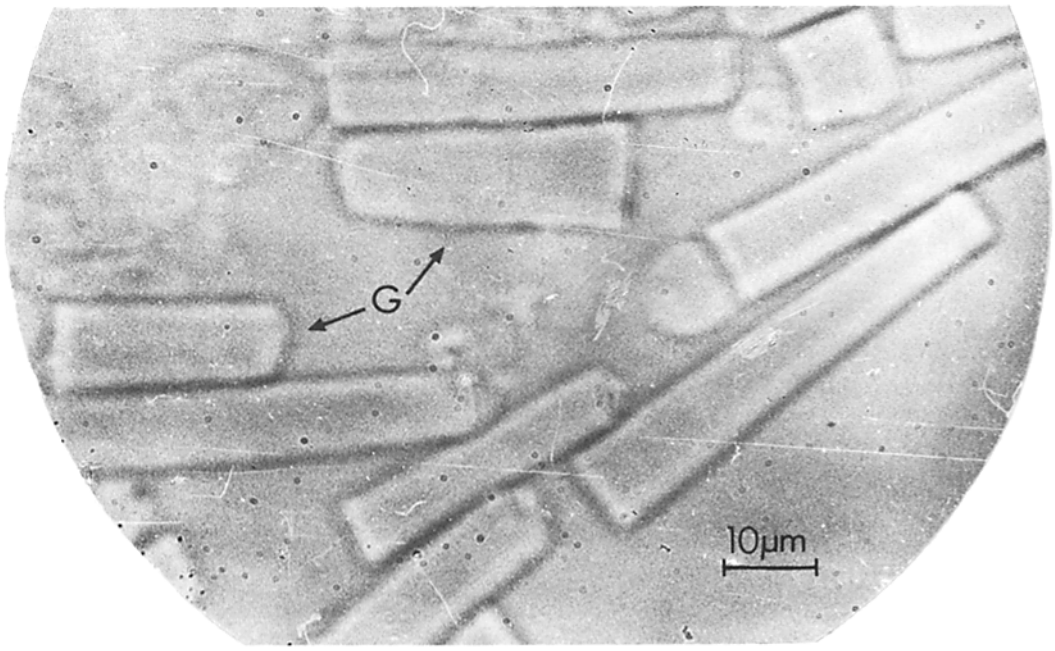

FIGURE 6. Photomicrograph of a retinal cell preparation of the tropical toad (*B. marinus*) at an enlargement of 1,250×, showing two green rod outer segments (G) amidst several red rod fragments.

of red rods of the adult salamander (Fig. 4 *a*) or leopard frog (Hárosi and MacNichol, 1974 *b*). The match between the normalized component and the rhodopsin standard of 502-nm peak is illustrated in part *b*; and again, the agreement between the curves should be less favorable due to the aforementioned reason (cf. Fig. 4 *b*). The half-band width was determined to be about 4,000 cm^{-1}, the average dichroic ratio, 4.06, and the uncorrected specific density, $0.0161/\mu m$.

The average absorption spectrum with its polarized components obtained from the conspicuous green rods is illustrated in Fig. 8 *a*. In part *b*, the normalized transverse component and the rhodopsin template with $\lambda_{max} = 433$ nm are shown, with the measured trace again exhibiting a considerable broadening as compared with the template, a phenomenon previously reported for *R. pipiens* frog and tadpole green rods by Liebman and Entine (1968). The half-band widths of the two components were estimated to be about 5,100 cm^{-1}, while the average dichroic ratio was determined to be 3.78 and the uncorrected specific density to be $0.0140/\mu m$.

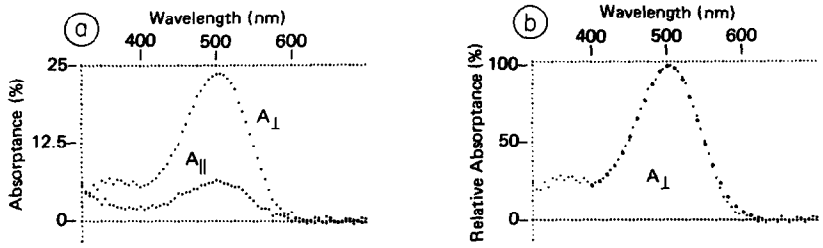

FIGURE 7. Polarized light absorption by transversely oriented dark-adapted red rod outer segments of the tropical toad (*B. marinus*). (*a*) The average of 10 single-cell recordings, each consisting of 32 bidirectional spectral scans. (*b*) The normalized transverse component (small filled circles) and a rhodopsin standard curve of 502-nm peak (large filled circles).

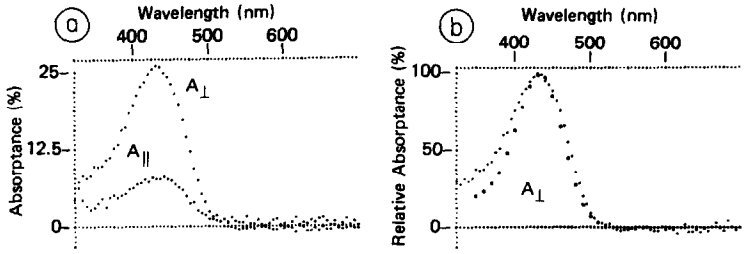

FIGURE 8. Polarized light absorption by transversely oriented dark-adapted green rod outer segments of the tropical toad (*B. marinus*). (*a*) The average of four single-cell recordings, each consisting of 32 bidirectional spectral scans. (*b*) The normalized transverse component (small filled circles) and a rhodopsin standard curve of 433-nm peak (large filled circles).

Synopsis of Measured Data

The cellular dimensions were obtained by photographing the field of view of the measuring microscope subsequent to the completion of spectral recordings in the specimens. By also periodically photographing a standard microscopic grid of known dimensions, the linear extent of images were derived. The length and apparent diameter of outer segments and the number of cells so measured are tabulated in Table I. Spectroscopic data are summarized in Table II, with figures in parentheses corresponding to an average ± 1 SD obtained during the averaging process. For details of technique, see Hárosi and MacNichol (1974 *b*). The new information presented in Table III consists of half-band width values corresponding to each spectral component (see Methods).

DISCUSSION

An Interpretation of Linear Dichroism

If a cylindrical photoreceptor is placed in a rectangular coordinate system so that its long axis of symmetry coincides with the z direction and its x-y projection is a circle, then its dichroic ratio is defined as the ratio of optical densities measured with the light polarized across the cell (in the x or the y direction) to that polarized along its axis (z direction). Thus, $R = D_{\perp}/D_{\parallel}$ and, by implication, this ratio is to be determined at λ_{max}.

TABLE I

AMPHIBIAN ROD OUTER SEGMENT DIMENSIONS BASED ON PHOTOMICROGRAPHS TAKEN IN THE DMSP

Cell type	Average length	No. of cells	Average diameter	No. of cells
	μm		μm	
Necturus maculosus				
Rod	28.0	12	9.7	12
Ambystoma tigrinum (aquatic phase)				
Red rod	26.2	18	11.9	18
Green rod	23.6	1	7.1	1
Ambystoma tigrinum (land phase)				
Red rod	31.1	8	9.8	8
Green rod	—	—	—	—
Bufo marinus				
Red rod	51.3	8	7.3	14
Green rod	32.9	4	9.3	4

Note: In case cell tapering was encountered, which often happened, the diameter was taken to be the arithmetic mean between the larger and smaller diameters of the cell along the central ½–⅔ of its length.

TABLE II

SPECTROSCOPIC DATA CONCERNING SEVEN TYPES OF AMPHIBIAN RODS

Cell type	No. in average	λ_{max} (± estim. margin of error)	Peak optical density*		Dichroic ratio*	Uncorrected transverse‡ specific density*
			$D_\perp$	$D_\parallel$		
		nm			$R = D_\perp/D_\parallel$	$OD/\mu m$
Necturus maculosus						
Rods	(10)	523±1	0.124093 (0.140484–0.108298)	0.039721 (0.044159–0.035328)	3.12 (3.18–3.07)	0.0128 (0.0145–0.0112)
Ambystoma tigrinum (aquatic phase)						
Red rods	(11)	516±2	0.143129 (0.161190–0.125790)	0.037866 (0.043924–0.031892)	3.78 (3.67–3.94)	0.0120 (0.0135–0.0106)
Green rods	(2)	433±4	0.081393 (—)	0.025773 (—)	3.16 (—)	0.0115 (—)
Ambystoma tigrinum, (land phase)						
Red rods	(6)	502±1	0.173346 (0.184227–0.162729)	0.038098 (0.041818–0.034409)	4.55 (4.41–4.73)	0.0177 (0.0188–0.0166)
Green rods	(2)	433±2	0.072783 (—)	0.020850 (—)	3.49 (—)	— (—)
Bufo marinus						
Red rods	(10)	502±1	0.117373 (0.125790–0.109116)	0.028935 (0.035328–0.022634)	4.06 (3.56–4.82)	0.0161 (0.0172–0.0149)
Green rods	(4)	433±2	0.130060 (—)	0.034409 (—)	3.78 (—)	0.0140 (—)

* Average ± 1 SD.

‡ Transverse specific density is the peak optical density of the cell, measured sideways with transversely polarized light, divided by the cell's diameter. The density figures are uncorrected for bleaching caused by the measurement.

TABLE III

SPECTRAL WIDTH DATA OF AMPHIBIAN ROD PIGMENTS

Cell type	λ_{max} (± Estimated margin of error)		Optical density of polarized comp. at λ_{max}	$\Delta\nu$ (± Estimated margin of error)
	nm			cm^{-1}
Necturus maculosus	523±1	$D_\perp$	0.124093	4,834±100
Rod		$D_\parallel$	0.039721	4,855±200
Ambystoma tigrinum (aquatic phase)				
Red rod	516±2	$D_\perp$	0.143129	4,930±100
		$D_\parallel$	0.037866	4,842±200
Green rod	433±4	$D_\perp$	0.081393	5,702±200
		$D_\parallel$	0.025773	6,048±300
Ambystoma tigrinum (land phase)				
Red rod	502±1	$D_\perp$	0.173346	3,973±100
		$D_\parallel$	0.038098	4,040±200
Green rod	433±2	$D_\perp$	0.072783	5,039±200
		$D_\parallel$	0.020850	5,174±300
Bufo marinus				
Red rod	502±1	$D_\perp$	0.117373	3,974±100
		$D_\parallel$	0.028935	4,443±200
Green rod	433±2	$D_\perp$	0.130060	5,084±200
		$D_\parallel$	0.034409	5,499±300

$\Delta\nu = |(10^7/\lambda_1) - (10^7/\lambda_2)|$ computed in cm^{-1} when λ_1 and λ_2 are measured in nm at 50% of α-band peak density.

A simple view of a vertebrate photoreceptor can be obtained by associating an electronic transition dipole moment vector with the chromophore of each visual pigment molecule. By further assuming an equal and fixed angular relationship of these vectors to exist with the tansverse x-y plane, oriented such as to contribute in the z direction but without preference with respect to the x or the y coordinate axes (Model I of Liebman, 1962; Hárosi and Malerba, 1975), an equality of the transverse extinction components, $E_x = E_y$, can be implied. When the total extinction is defined as $E = E_x + E_y + E_z$, the dichroic ratio becomes $R = E_x/E_z$ (if collimated light is used to measure the extinction components), and the z proportion of the moments may be written as

$$M_z = \frac{E_z}{E} = \frac{E_z}{2E_x + E_z} = \frac{1}{1 + 2R}. \quad (1)$$

Thus, Eq. 1 relates the cellular dichroic ratio to that fraction of each and every total transition moment that contributed in the z direction. Because noncollimated conditions prevail in microscope condensers, Eq. 1 needs to be

modified, becoming

$$M_z = \frac{1}{3 + 2\left(\frac{R - 1}{1 - bR}\right)}, \tag{2}$$

where $b = \tan^2(\alpha/2)$, with α the semiaperture of the condenser, and R the measured dichroic ratio (Hárosi and Malerba, 1975).

Using Eq. 1, Hárosi (1975 *b*) derived the relationship

$$(c\epsilon_{max}) = \left(\frac{1 + 2R}{3R}\right)\left(\frac{D_\perp}{l}\right), \tag{3}$$

which links the molar concentration c and extinction coefficient ϵ_{max} to the dichroic ratio R and the transverse specific density $D_\perp/l$. Similarly, by the use of Eq. 2, the following relation can be derived:

$$(c\epsilon_{max}) = \frac{[1 + R(2 - 3b)]}{3R(1 - b)}\left(\frac{D_\perp}{l}\right). \tag{4}$$

Since the optical parameters of the measuring instrument set the value of b, an oil immersion-type condenser of 0.4 numerical aperture yields $b = 0.0197$ (Hárosi and Malerba, 1975), and thus Eq. 4 for the DMSP becomes

$$(c\epsilon_{max}) = \frac{(1 + 1.941R)}{2.941R}\left(\frac{D_\perp}{l}\right). \tag{5}$$

Eq. 5, therefore, provides a method, accurate within the assumptions of the model, of assessing the product of molar concentration and extinction coefficient via the measured cellular parameters of transverse specific density and dichroic ratio.

Molar Extinction Coefficients of Rhodopsin and Porphyropsin

Since the initial determination of peak molar extinction (or molar extinction coefficient) of cattle rhodopsin (solubilized in 2% aqueous digitonin) at 40,600 liter/mol cm by Wald and Brown (1953), this quantity has been redetermined at 42,000 by Matthews et al. (1963) and Shichi et al. (1969), at 43,000 by Daemen et al. (1970), at 42,800 by Bridges (1971), and at 43,250 by Rotmans et al. (1972). Although other values (some being drastically lower) have also been reported, it is now commonly accepted that the peak molar extinction of cattle and frog rhodopsins is in the range of 40,000–43,000 liter/mol cm.

In sharp contrast with the large number of studies carried out on rhodopsins, the molar extinction coefficient of a porphyropsin appears to have been determined only once. Brown et al. (1963) reported (as a result of an unpublished work) 30,000 liter/mol cm for this coefficient when derived from the digitonin-

extracted visual pigment of the yellow perch (see, Note 4 by Dartnall, 1968). Although direct confirmation of this result is unavailable, the value of 30,000 as the molar extinction coefficient for some porphyropsins can be indirectly substantiated, as discussed below.

While studying the effect of hydroxylamine upon the photosensitivity of visual pigments, Dartnall (1968) discovered that they form two well-defined classes. The seven rhodopsins (with λ_{max} ranging from 486 to 520 nm) and the five porphyropsins (with λ_{max} ranging from 523 to 543 nm) that Dartnall measured yielded mean photosensitivities $(\epsilon\gamma)_{max}$ of 27,400 and 19,300 liter/mol cm, respectively. Although the quantum efficiency of bleaching γ is not known independently, it can be calculated from the photosensitivity figures if the peak molar extinctions of the pigments are known. Assuming ϵ_{max} = 42,000 liter/mol cm for the rhodopsins and ϵ_{max} = 30,000 liter/mol cm for the porphyropsins, γ = 0.652 results for the former and γ = 0.643 for the latter class. Thus, the similarity in γ, expected on various grounds, can be regarded as a validation of the above molar extinction coefficients, since the independently determined and strikingly different photosensitivities would otherwise be unlikely to converge (see Dartnall, 1968).

Another line of evidence supporting the relative magnitudes of peak molar extinctions of some visual pigments is provided by the microspectrophotometric measurements of Hárosi and MacNichol (1974 *a*, *b*), who found that the average transverse specific optical density of goldfish cone outer segments is proportional to the average transverse specific optical density of frog rod outer segments as ϵ_{max} = 30,000 of porphyropsin is to ϵ_{max} = 42,000 of rhodopsin (within an error of about 5%). Thus, as long as the *in situ* visual pigment arrangement and concentration remain nearly invariant, the MSP measurements of photoreceptors yield results consistent with those derived from digitonin extracts in the presence of hydroxylamine. The present study provides additional evidence in support of the constancy of pigment packing; moreover, it is arrived at independently by way of an unrelated hypothesis.

Oscillator Strength

The intensity of an absorption band is proportional to the area under the extinction vs. wave number curve of that band. By the same token, the theoretically meaningful oscillator strength f is also a measure of absorption intensity, being related to the same area as

$$f = 4.32 \times 10^{-9} \int \epsilon(\nu)\, d\nu. \qquad (6)$$

A simple method of calculating f consists of approximating the integral in Eq. 6 by the area of an isosceles triangle whose height is equal to the peak molar extinction ϵ_{max} and whose width at half this height is the spectral half-band

width $\Delta\nu$, according to

$$f \simeq 4.32 \times 10^{-9} \epsilon_{max} \Delta\nu, \quad (7)$$

(for references, see Hárosi and MacNichol, 1974 *a*).

In view of the fact that the Dartnall principle fails to account for the narrow spectrum ($\Delta\nu \simeq 3{,}600$ cm^{-1}) of the red-absorbing ($\lambda_{max} \simeq 625$ nm) dehydroretinal-based pigments, Hárosi and MacNichol (1974 *a*) proposed a modification thereof such that not the shape but the α-band oscillator strength within each pigment family be regarded invariant. This hypothesis, in effect, relaxes the rigid demands imposed by the two nomograms so that ϵ_{max} and $\Delta\nu$ need not both stay constant, merely their product.

Although Eq. 6 was derived for an isolated absorption band while visual pigment α bands are probably composed of two or more spectral components, rough estimates of f values for a rhodopsin and a porphyropsin can be obtained. For example, Eq. 7 results in $f_1 \simeq 0.726$ for a typical rhodopsin α band ($\lambda_{max} = 502$ nm) based on the literature value of $\epsilon_{max} = 42{,}000$ liter/mol cm and measured $\Delta\nu = 4{,}000$ cm^{-1} (see Table III, for adult salamander red rods). Similarly, Eq. 7 yields $f_2 \simeq 0.622$ for a typical porphyropsin α band ($\lambda_{max} = 523$ nm) when $\epsilon_{max} = 30{,}000$ liter/mol cm is used with $\Delta\nu = 4{,}800$ cm^{-1} (see Table III, for mudpuppy rods). The difference between f_1 and f_2 is probably significant despite the existing spectroscopic similarities of rhodopsins and porphyropsins (i.e., their absorption bands are rooted in substantially the same electronic origin).

Interpretations of Experimental Data

The summary of data presented in Table IV is intended to show the connection between the hypothesis of invariance of oscillator strength and the constancy of *in situ* pigment concentration. The hypothesis is used first (columns 1–2) to estimate the peak molar extinctions, ϵ_{max}. The equivalent specific densities ($c\epsilon_{max}$) are calculated next (columns 3–5). Finally, the concentration values c are derived (column 6) from the two former quantities (columns 2 and 5). Although the resulting mean concentration of about 3.5 mM is somewhat higher than the highest estimate thus far reported (Liebman, 1962; Liebman and Entine, 1968), it is impressive that this value is held within approximately $\pm 10\%$ for six types of cells, half of them containing porphyropsins and the other half containing rhodopsins.

To be sure, other interpretations could also be attempted. For example, one might suppose that the detected difference in transverse specific density of mudpuppy rods and adult salamander red rods is due entirely to a difference in pigment packing, favoring the latter type. However, this explanation would ignore the experimentally established dissimilarities between rhodopsins and porphyropsins in ϵ_{max} and $\Delta\nu$. Another argument would be to grant the 42,000-

TABLE IV

SUMMARY OF MEASURED AND COMPUTED DATA CONCERNING AMPHIBIAN RODS AND THEIR VISUAL PIGMENTS

Cell type	$\Delta\nu$*	ϵ_{max}‡	R§	$(D_\perp/I)$‖	$(c\epsilon_{max})$¶	c**
	cm^{-1}	*liter/mol cm*		*OD/cm*	*OD/cm*	*mmol/liter*
Necturus maculosus						
Rod‡‡	4,800	30,000	3.12	137	105.3	3.51
Ambystoma tigrinum (aquatic)						
Red rod‡‡	4,900	29,400	3.78	128	96.0	3.27
Green rod‡‡	5,800	24,800	3.16	123	94.4	3.81
Ambystoma tigrinum (land)						
Red rod§§	4,000	42,000	4.55	195	143.3	3.41
Green rod§§	5,100	32,900	3.49	—	—	—
Bufo marinus						
Red rod§§	4,000	42,000	4.06	177	131.6	3.13
Green rod§§	5,100	32,900	3.78	154	115.5	3.51

* Approximate half-band width (measured). Rounded off from the polarized spectral components in Table III.

‡ Approximate molar extinction coefficient (computed). Based on Eq. 7, for $f = 0.726$ (rhodopsins) or $f = 0.622$ (porphyropsins), as discussed in the text.

§ Mean dichroic ratio (measured). From Table II.

‖ Transverse specific density (measured). Corrected from Table II values by increases of 7% (porphyropsins) or of 10% (rhodopsins), as stated in Methods.

¶ Equivalent specific density computed by Eq. 5.

** *In situ* pigment concentration (computed).

‡‡ Assumed to contain pure porphyropsin-type pigment.

§§ Assumed to contain pure rhodopsin-type pigment.

and 30,000-liter/mol cm figures for ϵ_{max} of rhodopsin and porphyropsin but attribute the gradations in transverse specific density within each class to gradations in concentration. Again, this is an unattractive explanation for its failure of assigning any role to the differences in $\Delta\nu$.

On the other hand, the constancy of *in situ* visual pigment concentration appears plausible by supposing that there is a definite space in the transverse membranous structures of vertebrate photoreceptors made available for pigment molecules which, excepting abnormal conditions such as vitamin A deficiency, is always completely filled in the dark. This reasoning not only accounts for the experimental data of this and all relevant previous studies cited above but also justifies the oscillator strength invariance hypothesis. An important consequence of the latter is that the nomogram principle, heretofore considered valid for all visual pigments, can no longer be upheld. Instead of using two standard shapes, one for the rhodopsins and one for the porphyropsins, two standard areas (oscillator strengths) would appear to better fit the experimental facts in cases when λ_{max} is displaced in either direction sufficiently

far from the 500–520-nm region of the spectrum. Hence, visual pigment nomograms should be applied with circumspection to peaks with λ_{max} far from those of the pigments from which the nomograms were derived.

An Estimation of Physiological Spectral Sensitivities

The prediction of the physiological responsiveness of photoreceptors becomes possible with the knowledge of transverse specific density values. When light propagates exactly along the axis of a cell (the presumed physiological direction), it seems as if its electric vector would have the same chance of interacting with the transverse component of pigment absorption vectors as when it penetrates the cell side-on (perpendicular to the axis) with transverse polarization; thus, the equivalence between transverse and axial specific densities appears reasonable. Consequently, the total optical density of a photoreceptor along its axis could be obtained by multiplying together its transverse specific density and its outer segment length, yielding in turn the physiologically relevant parameter of total axial absorptance.

For example, using the corrected transverse specific density figures (Table IV) for *Bufo marinus* red rods (0.0177/μm) and green rods (0.0154/μm), and assuming the average length of outer segments to be 50–60 μm for red and 30–40 μm for green rods, then the total receptor densities (at λ_{max}) would be 0.89–1.06 and 0.46–0.62 optical density units, respectively. These peak density figures imply that the corresponding absorptance spectra and spectral sensitivity curves must broaden due to self-screening (e.g., Dartnall, 1957, 1962; MacNichol et al., 1973), a phenomenon actually invoked by Dartnall (1967 *b*) in his attempt to explain the wide spectral sensitivity curves obtained by Donner and Reuter (1962).

A reinterpretation would be in order, however, if the green rods of the crab-eating frog (*R. cancrivora*) investigated by Dartnall (1967 *b*), of the *R. temporaria* used by Donner and Reuter (1962), and of the *B. marinus* (in this study) all use the same visual pigment (which is the more probable, since Dartnall's best estimate of λ_{max} = 433 nm is identical with that reported herein). Since the peak density of the green rods is probably closer to 0.5 (by the foregoing analysis) rather than to 0.76 (assumed by Dartnall), self-screening would play a reduced role and the natural broadness of this pigment spectrum ($\Delta\nu \simeq$ 5,100 cm^{-1}) would be partly responsible for the broadness of the observed spectral sensitivity curves. Why Dartnall did not find the green rod pigment spectrum of *R. cancrivora* in his extracts any wider than his rhodopsin template ($\Delta\nu \simeq$ 4,200 cm^{-1}) is a question that remains to be answered. Nevertheless, Liebman and Entine (1968) also reported qualitatively similar broadenings for the green rod spectra of *R. pipiens* frogs and tadpoles, so that the phenomenon has thus far been found to occur in three species belonging to two orders

of the amphibian class, the urodele salamanders and the anuran frogs and toads.

A Model for In Situ Orientation of Chromophores

The trends revealed by the dichroic ratios among the various visual cells appear to be worthy of further study. For example, according to Table II, photoreceptors with rhodopsin-based pigments are more dichroic than porphyropsin-based counterparts, and cells with shortwave pigments (green rods) are less dichroic than those absorbing at longer wavelengths (red rods) in both classes. These observed differences, combined with available molecular information on the two visual chromophores found in nature, could be used as clues to their *in situ* arrangement.

In every known visual pigment of the animal kingdom, the light-catching molecule is either the aldehyde (or imine) of vitamin A_1 (retinal or retinylidine) or the aldehyde (or imine) of vitamin A_2 (dehydroretinal or dehydroretinylidine), serving as chromophore of the rhodopsins and porphyropsins, respectively. The essential difference between the pigments of those two families appears to be restricted to the chemical differences in the chromophores, manifested mainly in that dehydroretinal lacks 2 of the 28 hydrogen atoms of retinal and possesses instead an extra double bond in the six-membered ring (e.g., Wald, 1968). The recent X-ray determination of 11-*cis* and all-*trans* retinal crystal structures by Gilardi et al. (1971) and the theoretical calculations concerning the spectral characteristics of some retinal isomers by Honig and Karplus (1971) provide additional details about the molecular aspects of the prosthetic groups of visual pigments.

A stereo model of 11-*cis*, 12-*s*-*cis* retinal, as found in the crystalline state by Gilardi et al. (1971), is shown in Fig. 9 *a*. It was constructed out of Dreiding units (W. Büchi, Flawil, Switzerland) designed to maintain correct bond angles and proportionate interatomic distances. An important feature of this molecule appears to be the segmentation of its conjugated double bond system into three planes, the longest segment extending from C_6 to C_{13} and containing six π electrons. A second segment extends from C_{12} to oxygen (or nitrogen, in rhodopsin), containing four π electrons, while the shortest segment has only two π electrons between C_5 and C_6 and lies in the plane of the ring (whose puckering is disregarded at present).

The same model is illustrated in Fig. 9 *b* so that the plane defined by C_6–C_{13} coincides with the X-Y plane. In this position, the C_{12}–O portion of the molecule is found twisted downward ($-Z$ direction) and the C_5–C_6 bond of the ring twisted upward ($+Z$ direction). Since it is impossible to collapse the three segments of the molecule into any one plane, the transition moment is expected to lie outside the planes defined by any two of the three segments. The closest approach of most double bonds to a single plane (X-Y) seemingly oc-

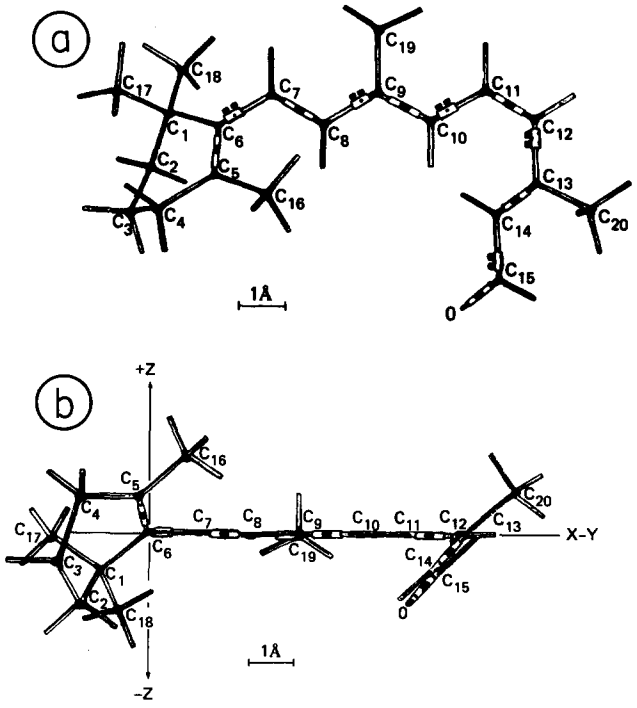

FIGURE 9. Perspective views of a stereo model of 11-*cis*,12-*s*-*cis* retinal, assembled according to the X-ray data of Gilardi et al., 1971. (*a*) As viewed from above. The unmarked free ends of rods and tubes represent centers of hydrogen atoms. The black junctions of the skeleton represent atomic nuclei of carbon (C_1–C_{20}). Double bonds are designated by two white bands separated by a black band. (The clamps appearing on five rods designating single bonds merely served to stabilize the model.) The black tip of the carbonyl group marks the position of the oxygen (O) nucleus. (*b*) As viewed from a point in the X-Y plane.

curs when the molecule is turned around C_6–C_{12} so that the average inclination of the C_{12}–O segment also coincides with the X-Y plane.

This position is shown in Fig. 10 *a*, indicating the proposed hypothetical orientation for rhodopsin-type pigment chromophores in vertebrate photoreceptors. Its relevance is based on two fundamental assumptions: first, that the electronic structure and conformation of 11-*cis*, 12-*s*-*cis* retinal in the crystalline state, as inferred by X-ray diffraction, closely resemble those of the chromophores of the rhodopsins and porphyropsins; and second, that the electronic transition dipole moment (corresponding to the main absorption band) has a spatial relationship with the atoms of the retinals that represents the average direction of travel of π electrons along the conjugated carbon atoms. Although these assumptions seem reasonable, unequivocal justification of their validity is in the uncertain future since the crystal structure of a native rhodopsin is yet to be determined. Nevertheless, the model is proposed as a working

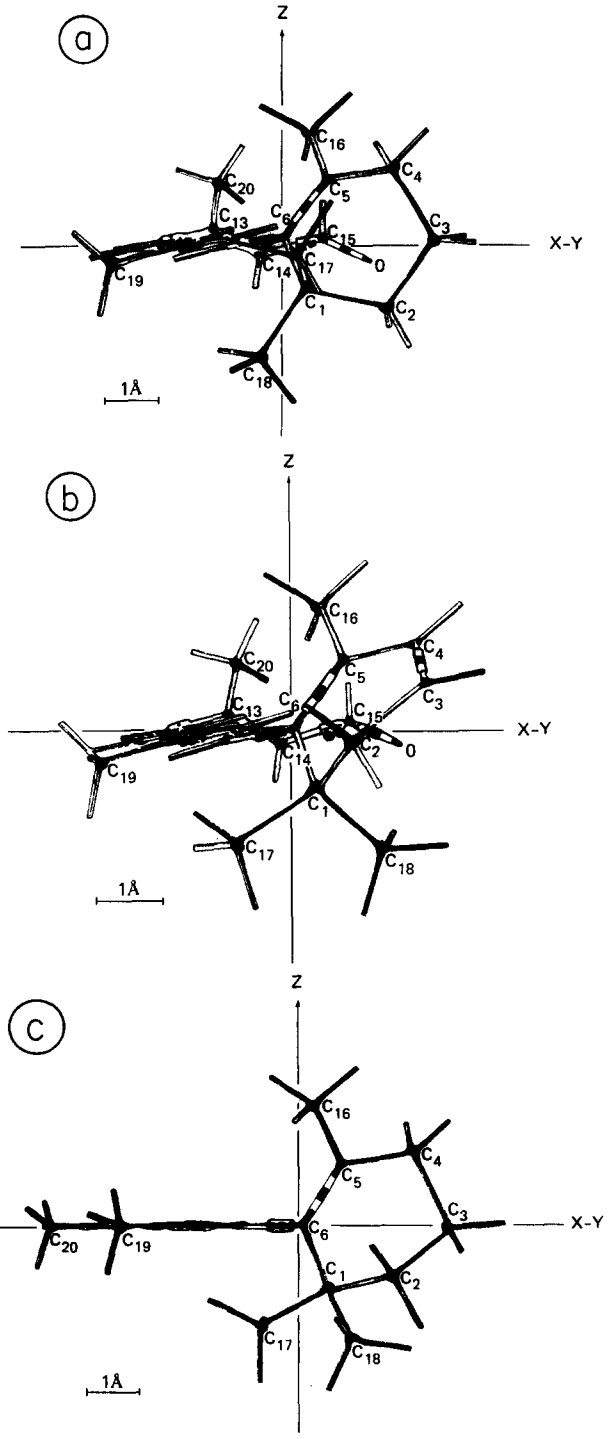

FIGURE 10

hypothesis, for it appears to enable the coherent interpretation of several seemingly unrelated experimental results.

For example, the main transition moment of the retinal molecule (Fig. 10 *a*) would be expected to incline to the X-Y plane at a small angle due to the orientation of the ring double bond ($C_5 = C_6$). This, in turn, could easily account for a 10% axial extinction of a rhodopsin-containing cell (by Eq. 1 for $R = 4.5$). On the other hand, if an extra double bond were added to the ring ($C_3 = C_4$) to lengthen the conjugation in the molecule, such as in dehydroretinal (Fig. 10 *b*), the transition moment would be expected to incline at a steeper angle with respect to the X-Y plane, easily causing a 14% Z contribution of a porphyropsin-containing cell (by Eq. 1 for $R = 3$).

Another aspect of the proposed retinal orientation concerns the observation (Hárosi and MacNichol, 1974 *b*) that photolyzed frog rod outer segments, although exhibiting a rapid spectral shift in λ_{max} from about 500 to 380 nm, maintain approximately the original dichroic ratio ($R = 4$–5) for a few seconds after the bleaching exposure. The model shown in Fig. 10 *c* was constructed according to the crystallographic data of all-*trans* retinal (Gilardi et al., 1971), which calls for an essentially planar side chain and a ring inclination to this plane of 59°. As it happens, the model is also consistent with the 11-*cis* retinals (Fig. 10 *a* and *b*) in that the orientation of their rings are nearly the same. On the basis of these models, therefore, photoisomerization might be expected to cause little change in the Z contribution of the transition moment and hence little change in dichroic ratio when the chromophore is switched from 11-*cis* to all-*trans*. The subsequent slow decline of transverse dichroism may occur by protein unfolding which could result in partial removal of constraints from the chromophore.

Thus, the proposed model for chromophore orientation is in harmony with the linear dichroism of dark-adapted and light-exposed vertebrate photoreceptors. Accordingly, since the ring portion of conjugation appears primarily responsible for axial absorption, the dehydroretinal-based pigments exhibit relatively high Z contribution and hence reduced dichroic ratio. The observation that green rods are less dichroic than red rods could be explained if the six-membered rings of the retinals in such pigments were twisted by more than

---

FIGURE 10. Proposed orientation of the retinals in vertebrate photoreceptors. (*a*) The model of 11-*cis*,12-*s*-*cis* retinal as viewed from a point in the X-Y plane located near the six-membered ring of the molecule. The X and Y directions signify the plane of the transverse membranes; the Z direction marks the axis of the cell. (*b*) The model of 11-*cis*,12-*s*-*cis* dehydroretinal in a similar view. Because of the added double bond ($C_3 = C_4$), the puckering of the ring is modified. (*c*) The model of all-*trans* retinal in bleached photoreceptors, shortly after photolysis. Except for puckering, the ring of this model assumes essentially the same orientation with respect to the X-Y plane as that of *a* and *b*.

40° with respect to the C_6–C_{13} segment. This situation, however, would imply a departure from the prevalence of the crystalline state conformation of the retinal molecules assumed above.

Further Inferences Derived from the Model

If isomerization of the retinals *in situ* causes no major change in ring orientation, then other portions of the molecule must move; thus, whereas the C_6–C_{12} segment may turn only slightly (by 10–20°) upon isomerization, the C_{13}, C_{14}, C_{15}, and the methyl C_{20} could suffer large dislocations. Observations upon the dichroism of photoproducts in frog rods (Hárosi, 1971; Hárosi and MacNichol, 1974 *b*) tend to support this interpretation in that transverse dichroism keeps declining as bleaching proceeds. Whereas metarhodopsin III exhibits only a slightly reduced dichroic ratio as compared with rhodopsin, subsequent products such as retinol or retinal oxime may be found with $R = 0.5$ to $R = 0.3$, which can be interpreted (by Eq. 1) as a change in Z contribution from the initial 10 to 50–60%. Thus, the transition moments associated with these chromophores would no longer be maintained at gently inclining angles to the X-Y plane. In view of the rotational freedom of single C–C bonds, the all-*trans* retinal molecules may in part turn out of the X-Y plane, causing the transition moments to be shifted to more acute angles.

The well-known fact that 9-*cis* retinal is accepted by opsin to form isorhodopsin suggests that the configurational requirement is not strict above C_{10}. Hence, it appears reasonable to suppose that bleaching, on the one hand, leaves the ring portion of the retinal and the C_6–C_{10} segment (with its two double bonds in the X-Y plane) essentially unchanged but, on the other hand, permits the rest of the molecule to turn (about the C_{10}–C_{11} bond) toward the Z direction. The slightly reduced dichroism of metarhodopsin III may be explained in an analogous fashion by assuming slight twists acting near the hydrophilic tip of the chromophore, whereas the purely hydrophobic portion of C_1–C_{10}, studded with four methyl groups, could be held by opsin by hydrophobic interactions.

The principles that follow from the proposed model appear compatible with Cone's (1972) conclusion that entire rhodopsin molecules float in lipid and undergo lateral or rotational diffusion about axes parallel with the Z direction. However, his suggestion of tumbling chromophores (i.e., rotation about axes in the X-Y plane) cannot easily be reconciled with the planar stability of transition moments associated with *in situ* visual pigments.

Another idea stemming from the model concerns the possible role of the various atomic groups of the retinals in the excitation process. If visual pigment chromophores are indeed anchored to opsin between C_1 and C_{10} and the C_{13}–C_{15} portion is relatively free to move, then the C_{20} methyl group attached to C_{13} may be considered as a strong candidate for the trigger portion

of the molecule (because of the large dislocation it undergoes during isomerization from 11-*cis* to all-*trans*). Although an understanding of what 11-*cis* retinal does to opsin upon absorbing a photon or what role the opsin plays in exciting photoreceptors is a long way off, even a tentative specification of the orientation of this molecule *in situ* may prove useful in the search for answers.

Received for publication 20 December 1974.

REFERENCES

BRIDGES, C. D. B. 1965. Absorption properties, interconversions, and environmental adaption of pigments from fish photo-receptors. *Cold Spring Harbor Symp. Quant. Biol.* **30**:317.

BRIDGES, C. D. B. 1967. Spectroscopic properties of porphyropsins. *Vision Res.* **7**:349.

BRIDGES, C. D. B. 1971. The molar absorbance coefficient of rhodopsin. *Vision Res.* **11**:841.

BROWN, P. K., I. R. GIBBONS, and G. WALD. 1963. The visual cells and visual pigment of the mudpuppy, *Necturus*. *J. Cell Biol.* **19**:79

CONE, R. A. 1972. Rotational diffusion of rhodopsin in the visual receptor membrane. *Nat. New Biol.* **236**:39.

CRESCITELLI, F. 1958. The natural history of visual pigments. *Photobiology. Oreg. State Univ. Biol. Colloq.* **19**:30–51.

CRESCITELLI, F. 1972. The visual cells and visual pigments of the vertebrate eye. *In* Handbook of Sensory Physiology, Vol. VII/1. Photochemistry of Vision. H. J. A. Dartnall, editor. 245–353. Springer-Verlag, New York.

DAEMEN, F. J. M., J. M. P. M. BORGGREVEN, and S. L. BONTING. 1970. Molar absorbance of cattle rhodopsin. *Nature (Lond.)*. **227**:1259.

DARTNALL, H. J. A. 1953. The interpretation of spectral sensitivity curves. *Br. Med. Bull.* **9**:24.

DARTNALL, H. J. A. 1957. The Visual Pigments. Methuen & Company, Ltd., London; John Wiley & Sons, Inc., New York.

DARTNALL, H. J. A. 1962. The photobiology of visual processes. *In* The Eye, Vol. 2. H. Davson, editor. Academic Press, Inc., New York. 323–533.

DARTNALL, H. J. A. 1967 *a*. *In* Color Science. G. Wyszecki and W. S. Stiles, editors. John Wiley & Sons, Inc., New York. 584.

DARTNALL, H. J. A. 1967 *b*. The visual pigment of the green rods. *Vision Res.* **7**:1.

DARTNALL, H. J. A. 1968. The photosensitivities of visual pigments in the presence of hydroxylamine. *Vision Res.* **8**:339.

DONNER, K. O., and T. REUTER. 1962. The spectral sensitivity and photopigment of the green rods in the frog's retina. *Vision Res.* **2**:357.

GILARDI, R., I. L. KARLE, J. KARLE, and W. SPERLING. 1971. Crystal structure of the visual chromophores, 11-*cis* and all-*trans* retinal. *Nature (Lond.)*. **232**:187.

HÁROSI, F. I. 1971. Frog rhodopsin in situ: orientational and spectral changes in the chromophores of isolated retinal rod cells. Ph.D. Thesis. The Johns Hopkins University, Baltimore, Maryland.

HÁROSI, F. I. 1975 *a*. Microspectrophotometry: the technique and some of its pitfalls. *In* Vision in Fishes: New Approaches in Research. M. A. Ali, editor. Plenum, New York. 43–54.

HÁROSI, F. I. 1975 *b*. Linear dichroism of rods and cones. *In* Vision in Fishes: New Approaches in Research. M. A. Ali, editor. Plenum, New York. 55–65.

HÁROSI, F. I., and E. F. MACNICHOL, JR. 1974 *a*. Visual pigments of goldfish cones. Spectral properties and dichroism. *J. Gen. Physiol.* **63**:279.

HÁROSI, F. I., and E. F. MACNICHOL, JR. 1974 *b*. Dichroic microspectrophotometer: A computer-assisted, rapid, wavelength-scanning phototometer for measuring linear dichroism in single cells. *J. Opt. Soc. Am.* **64**:903.

HÁROSI, F. I., and F. E. MALERBA. 1975. Plane-polarized light in microspectrophotometry. *Vision Res.* **15**:379.

HONIG, B., and M. KARPLUS. 1971. Implications of torsional potential of retinal isomers for visual excitation. *Nature (Lond.).* **229**:558.

LIEBMAN, P. A. 1962. *In situ* microspectrophotometric studies on the pigments of single retinal rods. *Biophys. J.* **2**:161.

LIEBMAN, P. A. 1972. Microspectrophotometry of photoreceptors. *In* Handbook of Sensory Physiology, Vol. VII/1. Photochemistry of Vision. H. J. A. Dartnall, editor. Springer-Verlag, New York. 481–528.

LIEBMAN, P. A., and G. ENTINE. 1968. Visual pigments of frog and tadpole (*Rana pipiens*). *Vision Res.* **8**:761.

MACNICHOL, E. F., JR., R. FEINBERG, and F. I. HÁROSI. 1973. Colour discrimination processes in the retina. *In* Colour 73, Proceedings for the Second Congress of the International Colour Association. Adam Hilger, Rank Precision Industries Ltd., London. 191–251.

MATTHEWS, R. G., R. HUBBARD, P. K. BROWN, and G. WALD. 1963. Tautomeric forms of metarhodopsin. *J. Gen. Physiol.* **47**:215.

ROTMANS, J. P., G. L. M. VAN DE LAAR, F. J. M. DAEMEN, and S. L. BONTING. 1972. On the molar absorbance of rhodopsin. *Vision Res.* **12**:1297.

SHICHI, H., M. S. LEWIS, F. IRREVERRE, and A. L. STONE. 1969. Biochemistry of visual pigments. I. Purification and properties of bovine rhodopsin. *J. Biol. Chem.* **244**:529.

WALD, G. 1945. The chemical evolution of vision. *Harvey Lect.* **41**:117.

WALD, G. 1968. The molecular basis of visual excitation. *Nature (Lond.).* **219**:800.

WALD, G., and P. K. BROWN. 1953. The molar extinction of rhodopsin. *J. Gen. Physiol.* **37**:189.

WALLS, G. L. 1963. The Vertebrate Eye and Its Adaptive Radiation. Hafner Publishing Co., Inc. New York.